Journal of Power Sources 397 (2018) 68–78

Contents lists available at ScienceDirect

Journal of Power Sources

journal homepage: www.elsevier.com/locate/jpowsour

Comparative study of Sn-doped $Li[Ni_{0.6}Mn_{0.2}Co_{0.2\text{-}x}Sn_x]O_2$ cathode active materials (x = 0-0.5) for lithium ion batteries regarding electrochemical performance and structural stability

M. Eilers-Rethwisch[a,b], S. Hildebrand[a,b], M. Evertz[a,b], L. Ibing[a,b], T. Dagger[a,b], M. Winter[a,b,c,**], F.M. Schappacher[a,*]

[a] *MEET Battery Research Center, Westfälische Wilhelms-Universität Münster, Corrensstr. 46, D-48149, Münster, Germany*
[b] *Institute of Physical Chemistry, Westfälische Wilhelms-Universität Münster, Corrensstr. 28/30, D-48149, Münster, Germany*
[c] *Helmholtz-Institute Münster, IEK-12, Forschungszentrum Jülich GmbH, Corrensstr. 46, D-48149, Münster, Germany*

HIGHLIGHTS

- $LiNi_{0.6}Mn_{0.2}Co_{0.18}Sn_{0.02}O_2$ exhibits an improved cycle life of about 20%.
- Lower transition metal dissolution in $LiNi_{0.6}Mn_{0.2}Co_{0.18}Sn_{0.02}O_2$.
- Decreased oxygen release during thermal decomposition due to a stronger Sn-O bond.
- Less heat evolution in the presence of electrolyte for Sn-doped cathode active material.

GRAPHICAL ABSTRACT

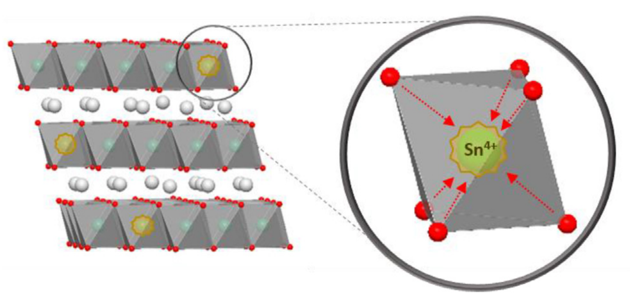

ARTICLE INFO

Keywords:
Lithium ion battery
Ni-rich NMC
Cycle life
Thermal analysis
Cationic substitution
Tin

ABSTRACT

Layered Ni-rich $Li[Ni_{0.6}Mn_{0.2}Co_{0.2\text{-}x}Sn_x]O_2$ cathode active materials with x = 0–0.05 are synthesized *via* a co-precipitation synthesis route and the effect of doping content on the structural behavior and electrochemical performance are investigated. All synthesized materials show a well-defined layered structure of the hexagonal α-$NaFeO_2$ phase (space group $R\bar{3}m$) analyzed by X-ray diffraction (XRD). Electrochemical Li-metal/cathode cell studies exhibit that a Sn-content of 1%–2% is beneficial regarding specific discharge capacity and cycle life ($\geq$20%). Detailed electrochemical investigations of Li-metal and lithium ion cells with cathodes consisting of $LiNi_{0.6}Mn_{0.2}Co_{0.2}O_2$ and $LiNi_{0.6}Mn_{0.2}Co_{0.18}Sn_{0.02}O_2$ are conducted. *Post mortem* analyses by means of ICP-OES and TXRF show beneficial effects of the Sn-doping with regard to a lower transition metal dissolution and a higher available Li content in the cathode active material. The thermal analyses (TGA, DSC, ARC) show a stabilizing effect of Sn-doping, which results from a lower mass loss and less heat evolution of the charged cathode active materials at elevated temperatures.

1. Introduction

In recent years, lithium ion batteries (LIBs) experience a surging demand with a dominant market share in portable electronics such as cell phones, tablet computers or power tools and progressively in electric vehicles and stationary battery storage systems ("grid

* Corresponding author. University of Münster, MEET Battery Research Center, Corrensstr. 46, D-48149, Münster, Germany.
** Corresponding author. University of Münster, MEET Battery Research Center, Corrensstr. 46, D-48149, Münster, Germany.
E-mail addresses: martin.winter@uni-muenster.de (M. Winter), falko.schappacher@uni-muenster.de (F.M. Schappacher).

https://doi.org/10.1016/j.jpowsour.2018.06.072
Received 29 January 2018; Received in revised form 30 May 2018; Accepted 18 June 2018
0378-7753/

batteries") [1]. LIBs became game-changers due to continuously major advancements in the lithium ion technology [2–4], which lead to higher energy densities and more power at lower cost [5–11]. However the advancements focusing solely on an increasing energy density can lead to new drawbacks, which include a decreased cycle life and safety issues, mostly due to structural instabilities of the negative (anode) [12] and positive (cathode) active materials [13–16]. The instabilities may result in the worst case in uncontrollable exothermic reactions that can eventually lead to a so-called thermal runaway of the battery cell [17,18]. For layered cathode active materials, the main reason that can trigger a thermal runaway, is the release of highly reactive oxygen due to phase changes at elevated temperatures and the subsequent reaction with the flammable organic carbonate-based electrolyte [19]. From this point of view, an improvement of the structural stability of cathode active materials, which have a high energy density, like nickel rich (Ni-rich) layered lithium-nickel-manganese-cobalt-oxides ($Li[Ni_xMn_yCo_z]O_2$ (NMC); $x + y + z = 1$) is indispensable to guarantee safe high energy cathode active materials [20–22]. One well-known method for stabilizing cathode active materials is doping. With doping, which rather means the substitution of cations in the host structure, the crystal structure can be modified specifically. Many studies have been conducted with Al [23–27], Mg [28,29], Ti [30,31], Cr [32], Ga [29,33], and Fe [26,27]. In NMC cathode active materials a substitution of Co is preferable. Ni is electrochemically active and provides most of the capacity and Mn, which is electrochemical inactive, maintains the structural stability [21]. The advantage of Sn lies in the high bond dissociation energy to oxygen (Sn-O; ΔHf_{298} = 548 (21) kJ mol^{-1}) [34] the similar ionic radius compared to Co (r_{Sn} = 69 p.m.; r_{Co} = 61 p.m.) [35] and it is non-toxic as well as cost-effective and thus a suitable candidate for the application in LIBs.

In our study, a Ni-rich NMC-622 ($LiNi_{0.6}Mn_{0.2}Co_{0.2}O_2$) cathode active material is investigated and structurally improved by Sn-doping. Previous investigations on doped cathode active materials have shown a beneficial effect on the thermal behavior. Nevertheless, doping contents larger than 5% can diminish the capacity [36,37]. Regarding this issue, the doping content of Sn ($Li[Ni_{0.6}Mn_{0.2}Co_{0.2\text{-}x}Sn_x]O_2$ with x = 0–0.05) is decreased step by step beginning with x = 0.05 down to x = 0.01 resulting in improved cycle life and enhanced thermal stability. The materials are synthesized *via* a pH-controlled co-precipitation synthesis route and are electrochemically and thermally investigated.

2. Experimental

2.1. Synthesis of active material and electrode preparation

Sn-doped $Li[Ni_{0.6}Mn_{0.2}Co_{0.2\text{-}x}Sn_x]O_2$ (x = 0–0.05) cathode active materials were synthesized *via* a co-precipitation method. As starting compounds $NiSO_4{\cdot}6H_2O$, $MnSO_4{\cdot}H_2O$, $SnSO_4{\cdot}H_2O$ (all from Sigma Aldrich, USA; purity ≥ 95%), $CoSO_4{\cdot}7H_2O$ (Acros, USA; purity ≥ 99%) and NaOH pellets (Sigma Aldrich, USA; purity ≥ 98%) were used. A 100 mL aqueous solution of metal sulfates in a stoichiometric ratio (total concentration equal to 2 M) and a 100 mL 2 M solution of NaOH (Fisher Scientific, USA; purity ≥ 97%) with a desired amount of NH_4OH-solution (Sigma Aldrich, USA; ~25% NH_3 based) were added continuously at a pH of 11 to a flask with 50 mL distilled water. After stirring 18 h the precipitate was filtered, washed several times with distilled water, and finally dried in air at 80 °C. The dried precipitate was ground in a mortar and then mixed with an excess (5%) of LiOH (Sigma Aldrich, USA; purity ≥ 98%) to compensate Li loss at temperatures over 700 °C and ground in a planetary ball mill from Fritsch (Germany; *Pulverisette 4 'classic line'*). The mixed materials were calcined in a muffle furnace from Nabertherm (Germany; *P300*) first at 480 °C for 5 h and finally at 850 °C for 10 h in air, yielding the desired products.

The active materials were mixed with Super C65 carbon black as conductive agent (Imerys, Switzerland) and a polyvinylidene difluoride binder (Solvay, Belgium; PVdF, *Solef 6020*) in a mass ratio of 90:5:5, dissolved in *N*-Methyl-2-pyrrolidone (33 wt% solid content; Carl Roth, Germany; NMP, purity ≥ 99%) and coated on an Al foil. The average mass loading of the electrodes was 3.7 (± 0.5) mg cm^{-2} with a dry film thickness of 90 (± 20) μm. In our lithium ion cell studies, graphite based anodes were used (Customcells, Germany; 1.4 mAh cm^{-2}). The area capacity of the cathode (~0.7 mAh cm^{-2}) was adjusted accordingly. After drying overnight in air at 80 °C, electrodes were punched and dried again under vacuum at 120 °C for 17 h to remove solvent residues. Before assembling 2032-type (Hohsen, Japan) coin Li-metal/cathode cells (Lithium from Albemarle, battery-grade, USA) in a dry room, the electrodes were pressed for 15 s with 8.5 tons. The electrolyte used was 1 M $LiPF_6$, in a mixture of ethylene carbonate and dimethyl carbonate (EC:DMC) [1:1 *wt.*] (BASF, Germany, *Selectilyte*). A six-fold non-woven polypropylene fleece (Freudenberg, Germany; *FS2226*) was used as separator.

2.2. Powder X-ray diffraction (XRD)

Powder X-ray diffraction measurements were performed with a D8 Advance device from Bruker (Germany) with a non-chromatic Cu-K_α-radiation (λ = 0.154 nm) in the 2θ range of 10°–90° in Bragg-Brentano geometry, to examine the synthesized materials for impurity phases and lattice constants, which were calculated using the TOPAS software (Bruker AXS, Germany; *Academic Version 4.2*).

2.3. Scanning electron microscopy (SEM) and energy dispersive X-ray spectroscopy (EDX)

Scanning electron microscopy and energy dispersive X-ray spectroscopy were carried out with a field emission gun (*Schottky-type*) from Zeiss (Germany; *Auriga CrossBeam*), which give an indication about the particle morphology of the active material and its composition. In addition, predictions of the distribution of the elements in the electrodes are possible. The energy dispersive analysis of X-rays was performed by an X-Max 80 mm^2 EDX detector from Oxford Instruments (United Kingdom).

2.4. Electrochemical investigations

Electrochemical charge/discharge cycling was performed with a Series 4000 Battery Tester from Maccor (USA) at 20 °C. The Li-metal/cathode studies were conducted in a two electrode set-up with two different procedures in the voltage range of 2.5 V–4.3 V. The first procedure included increasingly higher discharge rates (C/10, C/2, 1C, 5C; each for 5 consecutive cycles) with a constant current (CC) charge step of C/20 and subsequent cycling over 20 cycles with CC charge and a subsequent constant current/constant voltage (CCCV) discharge step until a rate of C/10 was reached. Within the second cycling procedure, the cycling stability was investigated until the discharge capacity decreased to 80% of its initial value, hereafter called a state of health (SOH) of 80% (SOH-80%). Herein, a CC charge step at 1C followed by a CV step until the current rate dropped below C/100 and a CC discharge step at 1C.

For cycling experiments of lithium ion cells, graphite anodes (Customcells, Germany) with an active material content of 96% and an area specific capacity of 1.4 mAh g^{-1} were used. The first charge step of the procedure started with a constant current rate of C/20 to a voltage of 4.2 V followed by a discharge step at C/10 to 3 V. The formation finished after four additional charge/discharge cycles at C/10. The 6th cycle consisted of a CC charge step at 1C followed by a CV step until the current rate dropped below C/20 and a CC discharge step at 1C. After the 7th charge, the cell was rested for 120 h (self-discharge step) followed by a CC discharge at a rate of 1C. Besides, the procedure includes two C-rate sequences between cycle 221–250 and cycle 461–490 including 5 cycles of CC at C/5, C/2, 1C, 2C, 3C and 5C, respectively. To